Pure & Appl. Chem., Vol. 57, No. 5, pp. 801–821, 1985.
Printed in Great Britain.

NMR of carotenoids—new experimental techniques

Gerhard Englert

Central Research Units, F. Hoffmann-La Roche & Co., Ltd., CH-4002 Basle (Switzerland)

Abstract - In continuation of my previous work further ^{1}H-NMR data of numerous end groups of retinoids and carotenoids are presented. In addition, the ^{13}C-NMR shifts and assignments of more than 60 end groups and derivatives thereof are compiled. Several new experimental NMR techniques which are extremely useful for the elucidation of molecular structures have been applied to carotenoids of known structure in order to demonstrate their utility and great power. Included are Double Indor Difference (DID) for the assignment of signals in complicated ^{1}H-NMR spectra, the pulse sequence DEPT for the investigation of the multiplicity of carbon signals, and some recent two-dimensional (2D) NMR techniques. Examples are given for the heteronuclear J-resolved 2D, the homonuclear (COSY) and heteronuclear chemical shift correlated 2D, and the 2D-INADEQUATE experiments. The last provides information on the carbon framework of the molecule. The advantages and disadvantages of these experimental techniques are discussed with special emphasis on the spectra of carotenoids.

INTRODUCTION

During the last three years again a number of new or improved NMR techniques has been made available to the practicing spectroscopist which will no doubt further enhance the importance and efficiency of NMR in solving complicated structural problems. It is the main objective of this paper to present some selected examples of the application of such new techniques in order to demonstrate and discuss their relative advantages and drawbacks with special emphasis on the spectra of carotenoids. In this context the following methods will be discussed:

- A simple modification of the long-known INDOR experiment called Double Indor Difference (DID) which significantly simplifies the assignment of proton signals in strongly overlapping spectra typical for carotenoids.
- A pulse sequence called DEPT, which is frequently applied now in ^{13}C-NMR spectroscopy to determine the multiplicity of the signals, i.e. the number of attached protons.
- Several two-dimensional (2D) NMR methods which were found extremely useful in the NMR of carotenoids. Although these methods are in part highly sophisticated from an experimental as well as a theoretical point of view, there is no doubt that they will be increasingly applied in this field in the near future. Due to lack of space and time I shall be unable, unfortunately, to discuss the physical background of these new methods and will merely reference the pertinent literature.

NMR DATA OF END GROUPS

Spectroscopic methods such as UV, MS and NMR are well-known, effective tools for the elucidation of the structure of carotenoids. An important starting point in this task, namely the determination or identification of the structure of the specific end groups, can be very efficiently achieved by ^{1}H- or ^{13}C-NMR. I previously presented ^{1}H-NMR data on 48 end groups with 84 derivatives including some cis isomers (Ref. 1). In Table 1 are shown further ^{1}H-NMR shifts for 26 additional end groups and 52 derivatives; thus data are now compiled for more than 70 different end groups and 136 derivatives.
Since ^{13}C-NMR has also become increasingly applied in the field of retinoids and carotenoids a similar compilation of ^{13}C chemical shifts is given in Table 2, containing 92 derivatives of 62 end groups. The data of Tables 1 and 2 were extracted from numerous spectra of retinoids and carotenoids which were all run and assigned in our laboratory. However, I should like to mention here that part of the data resulted from a very fruitful cooperation

Table 1. Characteristic ^{1}H-NMR data of some typical end groups of natural and synthetic carotenoids (solvent $CDCl_3$).*

(1c) 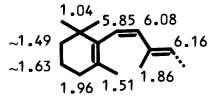	(5e) 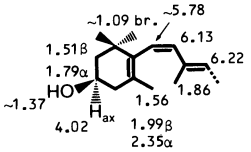	(5f) 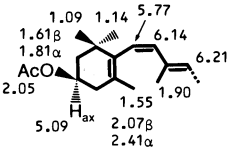	(14a) 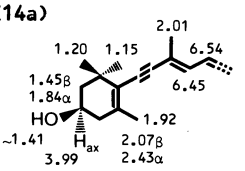
(14b) 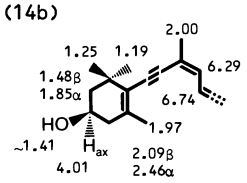	(14c) 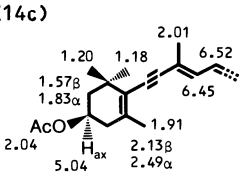	(14d) 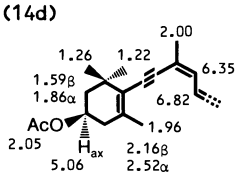	(43b) 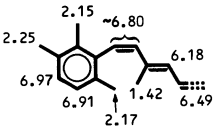
49a 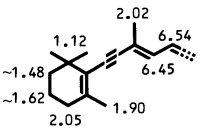	49b 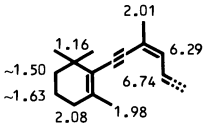	50 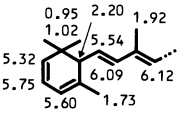	51 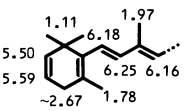
52 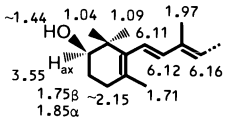	53 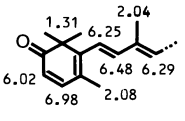	54a 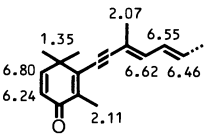	54b 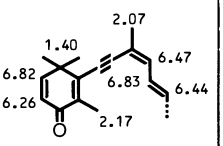
55 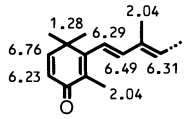	56a a) 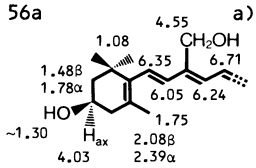	56b a) 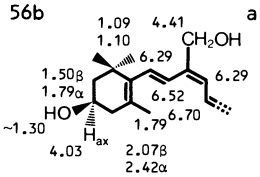	57a b) 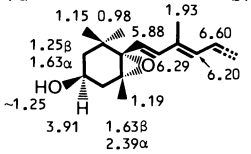
57b b) 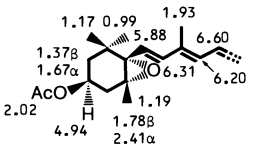	57c 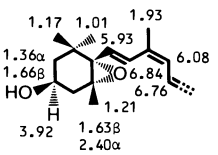	58a b) 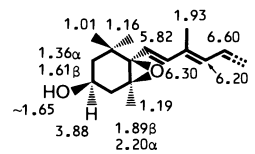	58b 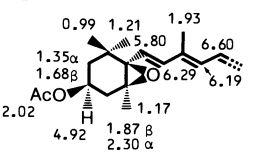
59a 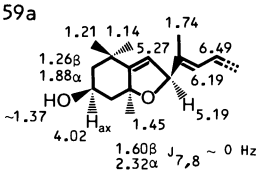	59b 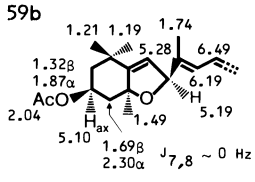	60a 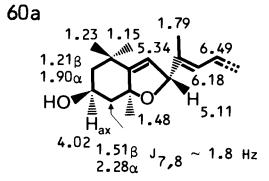	60b 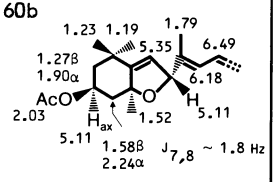

Table 1. Continued

61a b) 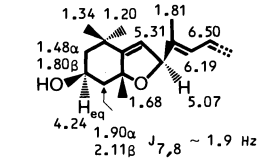	61b 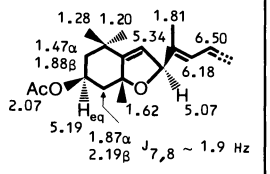	62a b) 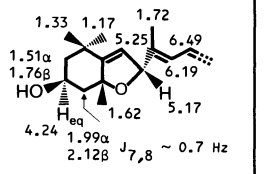	62b 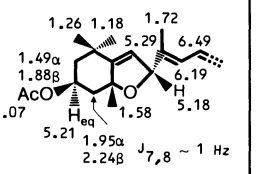
63 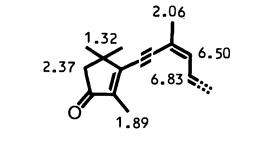	64 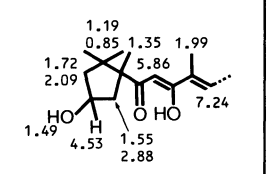	65 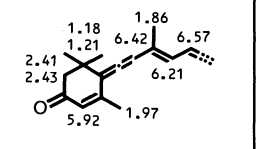	66a 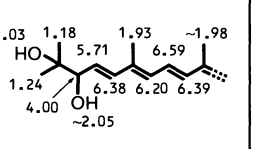
66b 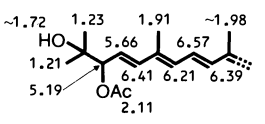	67a 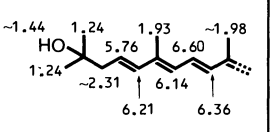	67b 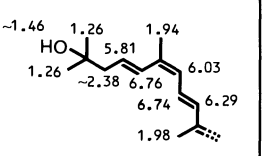	68 c) 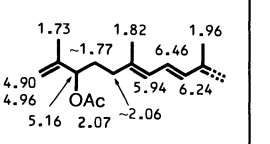
69a 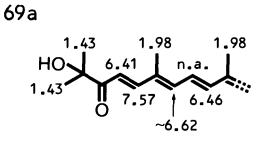	69b 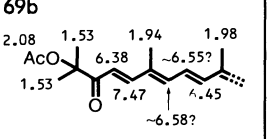	70 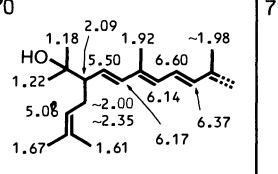	71 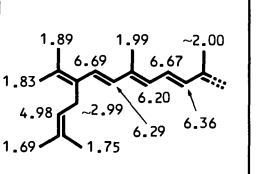
72a 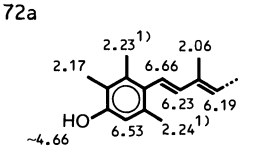	72b 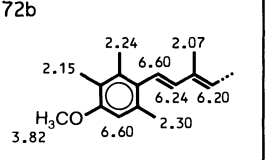	72c 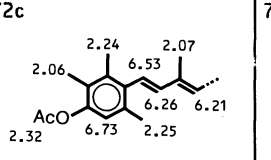	73a 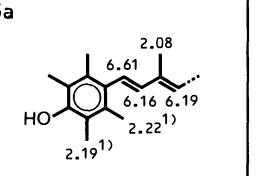
73b 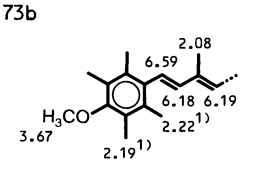	73c 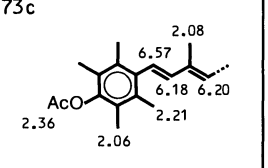	74a 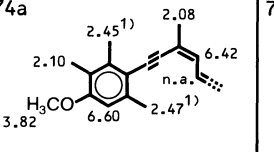	74b 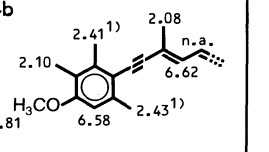

*Numbering continued from Table 1 of Ref. 1. Numbers in parantheses are supplements to the previous Table; [i)] corresponding assignments may be interchanged; br. broad signal, temperature dependent; n.a. not assigned. Note a): see Ref. 2. Note b): see Ref. 3. Note c): see Ref. 4.

Table 2. Characteristic ^{13}C-NMR data of some typical end groups of natural and synthetic carotenoids (solvent $CDCl_3$).

1a 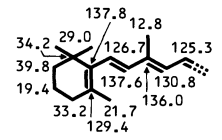	1b 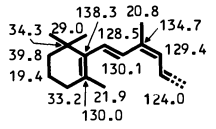	1c 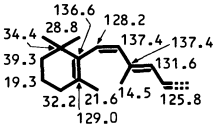	2 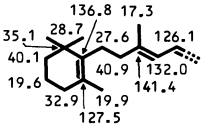
3 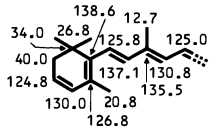	4 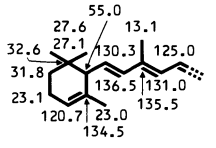	5a 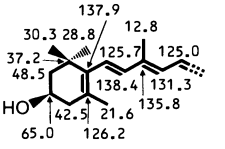	5b 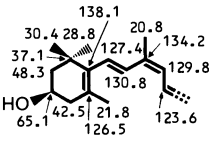
5c 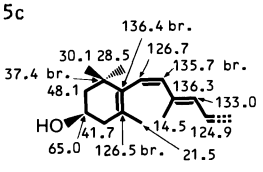	5d 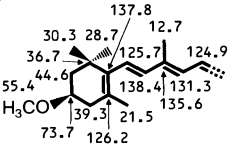	5e 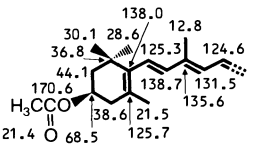	5f 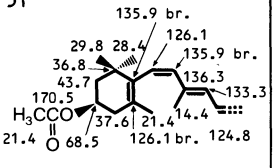
6a 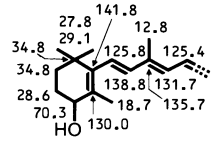	6b 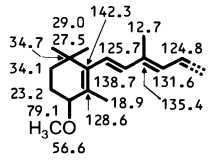	6c 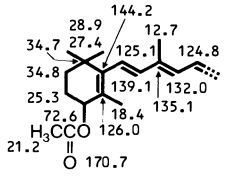	7 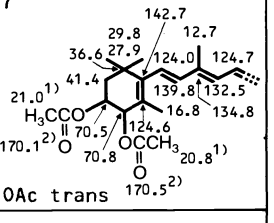 OAc trans
8 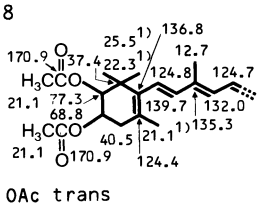 OAc trans	9 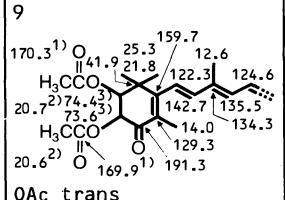 OAc trans	10 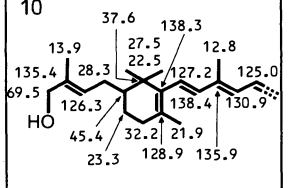	11 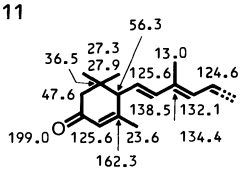
12 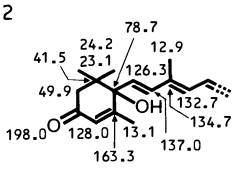	13 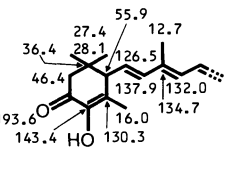	14 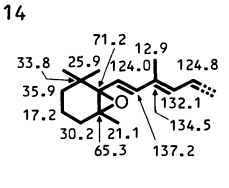	15 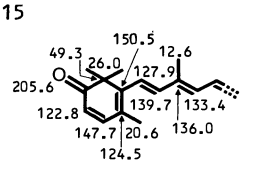

Table 2. Continued.

16

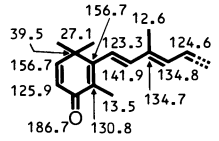

17a

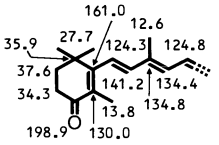

17b

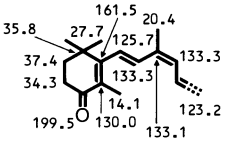

17c

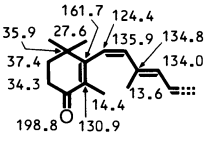

18a

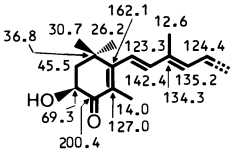

18b

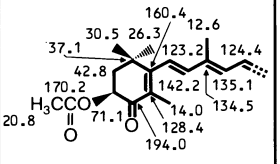

19a

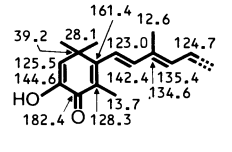

19b

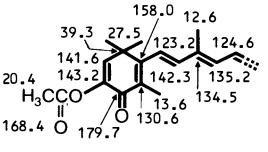

20

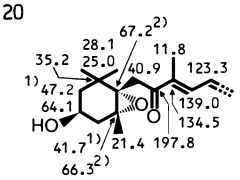

21

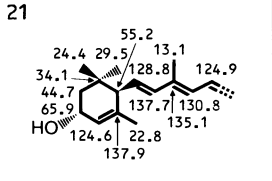

22

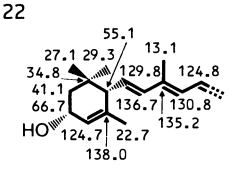

23

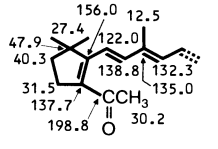

24

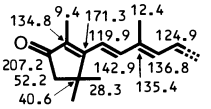

25

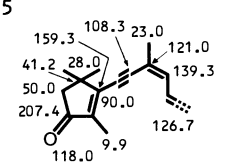

26

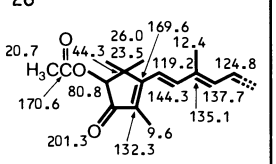

27a

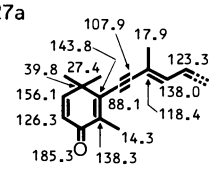

27b

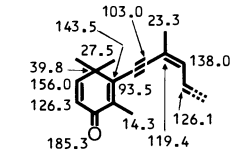

28

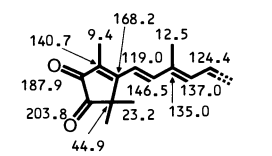

29

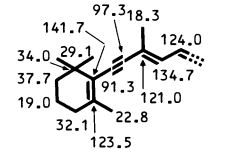

30a

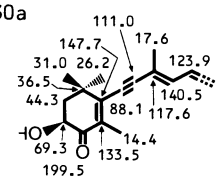

30b

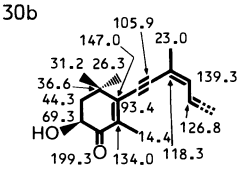

30c

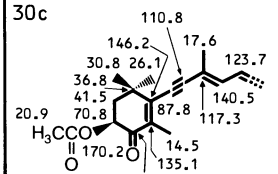

30d

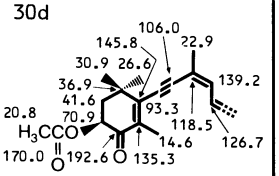

31a

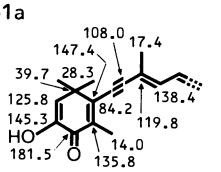

Table 2. Continued.

31b 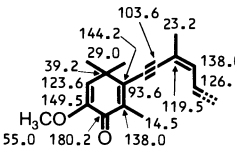	32 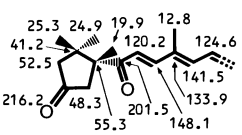	33a 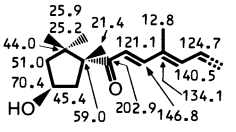	33b 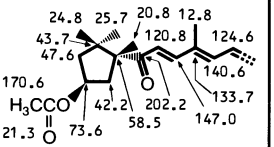
34a 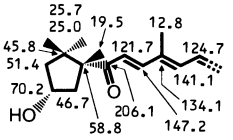	34b 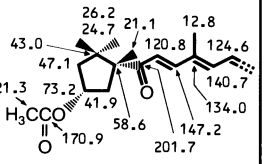	35a 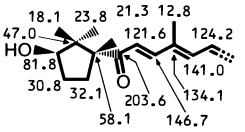	35b 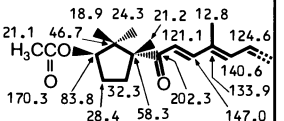
36 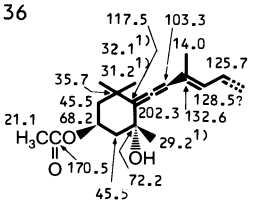	37a 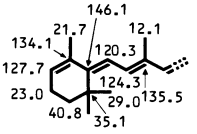	37b 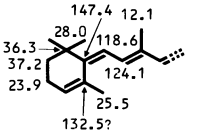	38a 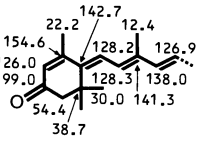
38b 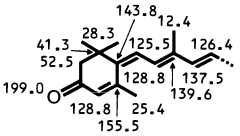	39 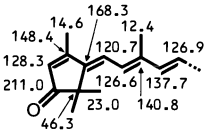	40 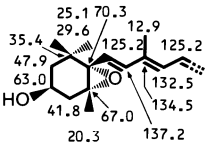	41a 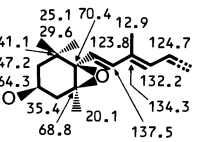
41b 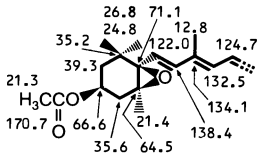	42 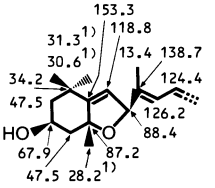	43 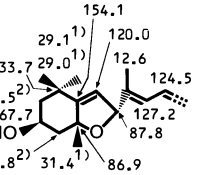	44 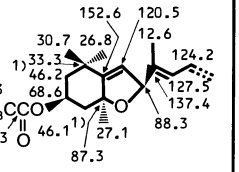
45 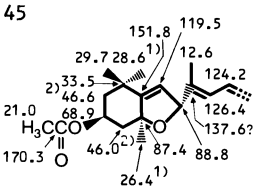	46 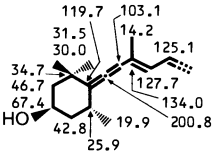	47 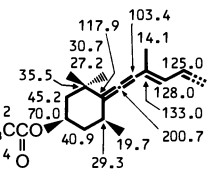	48a 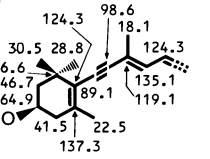

Table 2. Continued.

48b	48c	48d	49
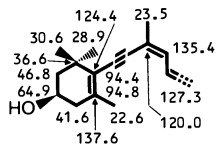	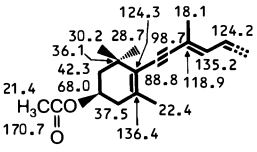	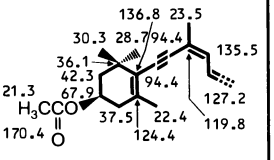	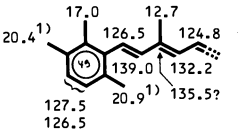
50a	50b	50c	51
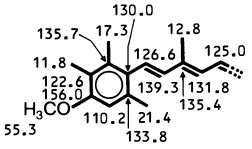	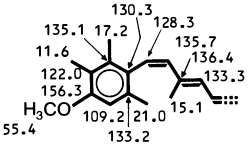	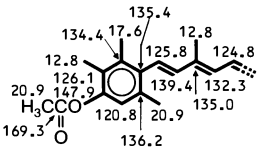	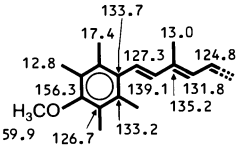
52a	52b	53	54
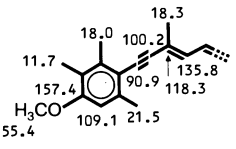	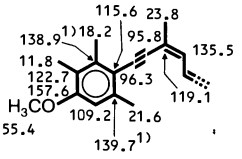	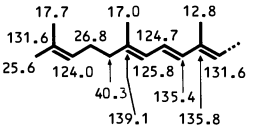	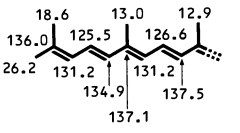
55	56	57	58
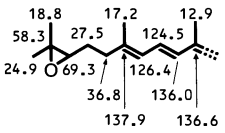	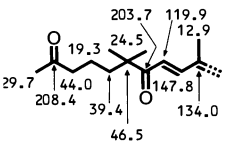	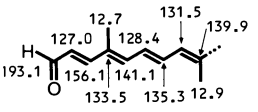	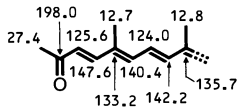
59	60	61	62
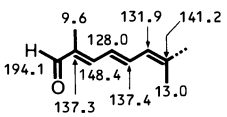	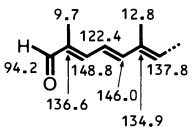	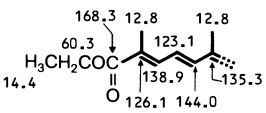	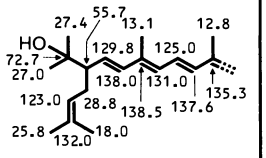

i) Corresponding assignments may be reversed.

with the groups of Dr. Britton (Liverpool), Prof. Eugster (Zurich), Prof. Jensen (Trondheim), Prof. Kleinig (Freiburg i.Br.) and Dr. Pfander (Berne), who kindly provided quite a number of interesting samples.
The assignments given in Table 1 were supported by the comparison of a great number of reference spectra, by decoupling and DID experiments (see example below) and by numerous homonuclear Overhauser difference experiments, a few examples of which were discussed previously (Ref. 1). Similarly, the assignments in Table 2 were based on the application of shift reagents, measurement of CW-offset and ^{1}H-coupled spectra (see Refs. 5, 6), and in several cases on the application of ^{13}C-^{1}H chemical shift correlated 2D experiments (see example below). In both Tables the chemical shifts of the first protons or carbons of the side-chains were included because they give additional information on the specific end group. Since these data were partly extracted from the spectra of retinoids and related compounds with only 4 or 5 conjugated double bonds the shifts of protons H(10) and H(11) as well as of carbons C(9) to C(11) had to be corrected in some of these cases by simple additivity rules in order to take into account the influence of strongly anisotropic terminal groups such as carbonyls or carboxyls.
The assignments were given as complete as possible and were carefully checked for consistency within the entire set of spectra available in our laboratory.
I hope that this extended chemical shift compilation will be of practical use in the identification of retinoids and carotenoids.

NEW EXPERIMENTAL TECHNIQUES

Double Indor Difference - Recently, the utility of the interproton Overhauser difference technique for the assignment of proton signals of carotenoids and the solution of stereochemical problems was strongly emphasized (Ref. 1). In this technique a sufficiently isolated signal (singlet or multiplet) is strongly irradiated for a few seconds by a second radiofrequency. After switching off the irradiation, the observation pulse is applied and the free induction decay (FID) is accumulated as usual. If a second FID is subtracted with the pre-irradiation set outside the absorption range the difference spectrum contains only those signals which have altered intensities in the two FID's. Signals with increased (positive) intensities are caused by the Overhauser effect and reflect a close spatial proximity of the two protons.
The long-known Fourier INDOR difference experiment (Ref. 7) uses a similar experimental set-up, however, only a short ($\leq$ 0.5 sec) and very weak ($\tilde{\gamma} H_2 \sim 1$ Hz) pre-irradiation is applied to one selected component of a multiplet. This causes a change of the population of these two energy levels which is reflected by a change in intensity of all other transitions which start or end on one of the two previous levels. In the INDOR difference spectrum only these so-called connected transitions within a coupled spin system appear as positive or negative signals reflecting an increase or decrease of the excess population of the corresponding transitions. The observation of these difference signals allows one to locate approximately the signals of coupled protons. The main advantage of INDOR is the fact that in contrast to decoupling or Overhauser experiments the perturbation is selectively applied only in a very narrow frequency range of the order of 1 Hz. This strongly extends the applicability of the method in crowded spectra.
Kessler and co-workers recently proposed a simple modification of the INDOR difference experiment called Double Indor Difference (DID; Ref. 8). A first modification is that the difference FID is obtained from two on-resonance experiments, namely by irradiating two suitably chosen components of a given multiplet, e.g. the first and second component of a doublet, or the first and fourth component of a doublet of doublets. The second modification is that instead of positive and negative signals, only positive ones are produced by applying a magnitude calculation to the final difference spectrum. The main advantage of DID is the fact that in simple, coupled spin systems as frequently observed in carotenoids the true multiplet structure of the coupled protons appears in the difference spectrum. As will be shown, this method greatly simplifies the assignment of protons in crowded spectra of carotenoids.
As an example shown in Fig. 1, DID is used to perform or confirm some assignments in the olefinic part of the 400 MHz spectrum of (5'R)-cryptocapsone (Ref. 6). As usual the assignments of the protons near the end groups are easily and unambiguously performed by comparison with the data of the two symmetrical compounds ß-carotene and (5R,5'R)-capsorubone (see Tables 1 here and in Ref. 1). These comprise H(7), H(8), H(10), H(14), H(14') and H(8'). Additional assignments can be obtained by a few selected DID experiments. The first experiment, namely pre-irradiation of H(8') near 7.4 ppm as indicated by the two arrows, results in the appearance only of the doublet for H(7') near 6.5 ppm. Irradiation of the first and fourth component of the doublet of doublets near 6.7 ppm gives rise to a further doublet of doublets and the broadened doublet of H(14), thus the two former multiplets must be assigned to H(15) and H(15') as it is confirmed by the fourth and sixth experiment. In the third experiment the signals of H(11), H(12) and H(10) are linked. From these and the fol-

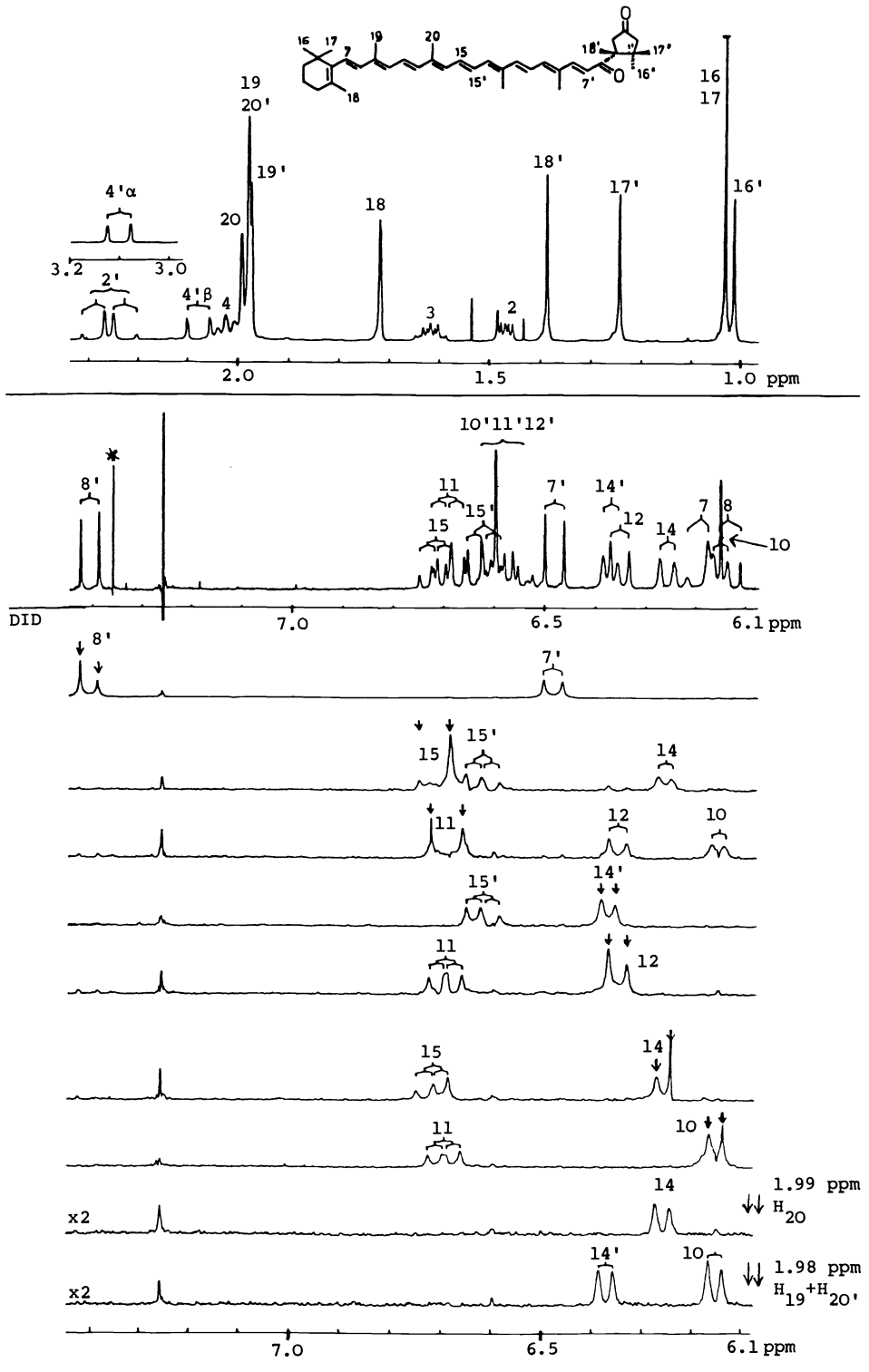

Fig. 1. Top: High and low-field sections of the 400 MHz ^{1}H-NMR of (5'R)-cryptocapsone in $CDCl_3$. Below: Sequence of DID experiments with pre-irradiation of 0.5 sec duration at positions marked by arrows; *impurity.

lowing experiments it is seen that by a series of DID experiments all but one sub-group of three coupled protons can be easily identified. These are the three very strongly coupled protons H(10'), H(11') and H(12') all absorbing near 6.6 ppm as revealed by the integral. It is worthwile mentioning here that DID can also be successfully applied to detect connectivities between the protons of the in-chain methyl groups and their olefinic coupling partners although the corresponding 4-bond coupling is only ca. 1.3 Hz. This is demonstrated in the last two experiments of Fig. 1. A difference spectrum obtained by pre-irradiation of the methyl signal at 1.992 ppm (H(20)) just before and after the peak maximum (difference ca. 1 Hz) gives rise to the appearance of the signal of H(14). Similarly, pre-irradiation of the 6-proton singlet near 1.98 ppm reveals connectivities of the corresponding methyl protons H(19) and H(20') with H(10) and H(14') leaving the assignment of the signal of the remaining in-chain methyl protons H(19') at slightly higher field.
In conclusion it is seen that DID is a very selective method for locating the signals of coupled spin systems in strongly overlapping spectra as those of carotenoids. Assuming normal sample quantities of a few mg a fully automated sequence of experiments can be performed in less than one hour (see example of Fig. 1). If longer accumulation times are acceptable, experiments in the µg-range are also possible. We have found that a few selected DID experiments which can be performed even on older instruments can replace, in certain cases, a much more time-consuming and complicated 2D experiment.

DEPT - The assignment of ^{13}C-NMR signals to the corresponding carbons in complicated molecules relies heavily on the correct determination of their multiplicities reflecting the number of directly attached protons. This information was previously derived from proton coupled spectra or from CW-offset decoupled spectra. The former method gives additional information on the proton-carbon couplings J_{CH}, the latter on relative chemical shifts of the corresponding protons if the magnitude of the couplings are roughly predictable. However, it is frequently difficult, even at high magnetic fields, to identify the different multiplets in crowded spectra and hence reliably to derive the individual multiplicities. In addition, a considerable loss of intensity is implied due to the splitting of the carbon signals into several components; thus much longer acquisition times are needed.
In the last few years a number of multi-pulse sequences has been proposed for the rapid determination of the multiplicities of ^{13}C signals (Refs. 9, 10). For almost two years we have routinely applied the pulse sequence called DEPT (Distortionless Enhancement by Polarization Transfer; Ref. 10) which has several advantages compared to previous methods (Ref. 11). In this technique which uses two carbon-13 and three proton pulses, polarization is transferred from protons to carbons, i.e. the excess population between the ^{13}C levels and hence the intensity of these transitions is enhanced considerably, thus reducing the acquisition time. The separating delay between the pulses is set equal to $1/(2J_{CH})$. This one-bond ^{13}C-^{1}H coupling may vary in carotenoids between ca. 130 and 170 Hz. A further advantage of DEPT is that the results do not critically depend on the value used for J_{CH} and therefore a typical average value of ca. 140 Hz is suitable. If the usual broad-band proton decoupling is switched on during the accumulation of the FID, the intensity of the decoupled ^{13}C singlets depends on the magnitude of the last proton pulse in the pulse sequence, called theta pulse P_θ, and on the number of protons attached to the carbons. This dependence is caused by the different rotation frequencies and phases of the transverse magnetizations of the different types of carbon-13 due to the couplings to the attached protons (Ref. 10).
A typical example is shown in Fig. 2 wherein trace A represents the normal ^{13}C NMR spectrum of astaxanthin diacetate, the assignments of which are known (Ref. 1). Also presented is a set of typical DEPT spectra obtained for 90° (trace B), 45° (trace C) and 135° theta pulses (trace D). The first observation is that in all these DEPT spectra the quaternary carbon signals (designated by s in trace A) including the solvent signals are eliminated. In addition, in trace B only CH signals are retained, in trace C all protonated carbons are seen with positive intensities, in trace D CH and CH_3 are positive, CH_2 negative. Thus, the clear-cut differentiation of all the signals according to their multiplicities is possible even in very crowded spectra. The normal ^{13}C-NMR was obtained from 128 scans, the DEPT spectra from 256 scans with a relaxation delay of 4 sec. It is clearly seen that only a small fraction of this number of scans is actually needed for a signal-to-noise ratio comparable to the normal spectrum.
Useful for daily routine applications is the fact that, in general, a single experiment, namely the one in trace D (P_θ = 135°), is sufficient to give all needed information, if the CH and CH_3 signals can be differentiated by consideration of their chemical shifts at low and high field, respectively.
However, if all three DEPT spectra are available one can calculate linear combinations of the three spectra yielding so-called edited DEPT spectra presenting separated sub-spectra for all three types of carbon as shown in Fig. 3. Thus, trace C of Fig. 3 with the CH_2 sub-spectrum was obtained by substracting trace D from C of Fig. 2 with a suitable scaling factor. Similarly, the CH_3 sub-spectrum was calculated from all three spectra of Fig. 2.

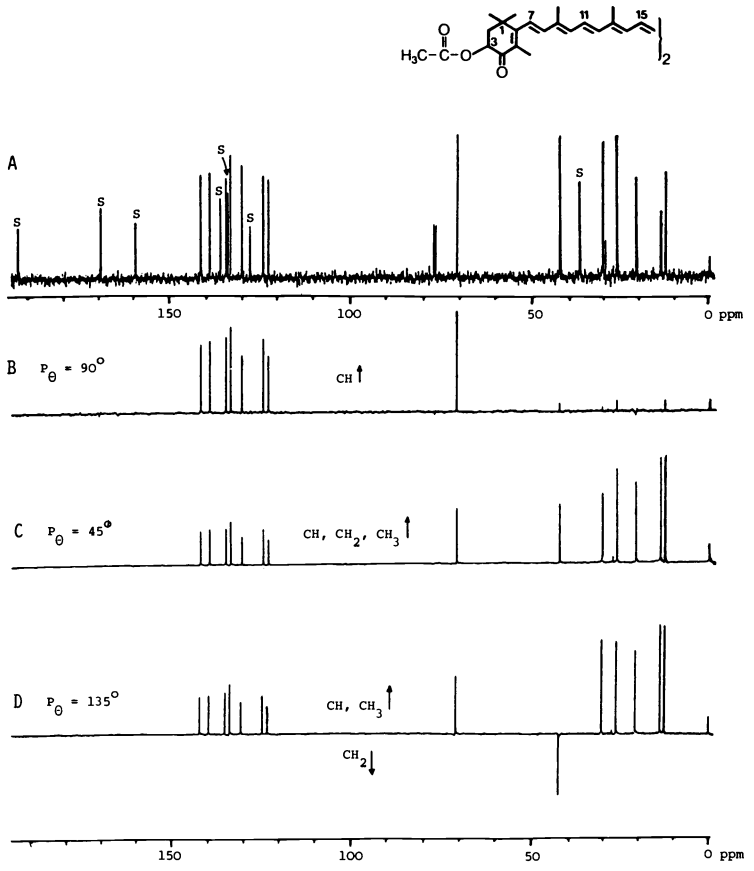

Fig. 2. A: 100 MHz ^{13}C-NMR of astaxanthin diacetate (60 mg in 0.4 ml $CDCl_3$, 128 scans, 45° flip angle); S quaternary carbons. B,C,D: DEPT spectra obtained for proton pulses P_θ = 90°, 45° and 135°; 256 scans, 4 sec relaxation delay, J_{CH} ~ 130 Hz.

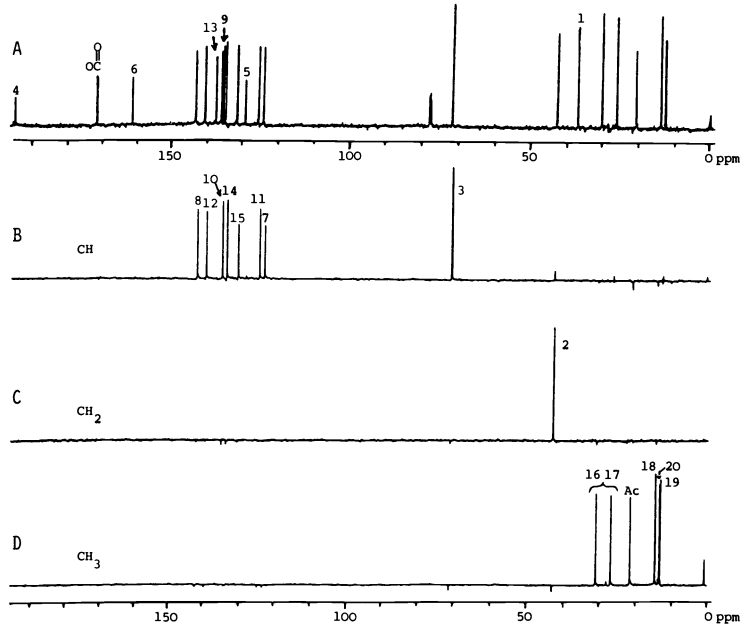

Fig. 3. 100 MHz ^{13}C-NMR and edited DEPT spectra of astaxanthin diacetate.

It should be mentioned that the DEPT sequence can be used also for the measurement of proton-coupled ^{13}C-spectra if the decoupler remains switched off during the accumulation of the FID. Several other pulse sequences have been published including those for the generation of ^{13}C sub-spectra of quaternary carbons only (Ref. 12). This might be useful in cases where quaternary and other carbons have exactly identical chemical shifts.

Two-dimensional NMR (2D) - The basic idea of 2D NMR was first proposed in 1971 by J. Jeener (Ref. 13). In more recent years this promising technique was mainly developed and extended by the research groups of R. Ernst and K. Wüthrich in Zurich and R. Freeman in Oxford (for an introduction see Ref. 14).
In a normal 1D Fourier experiment a short rf-pulse is applied to the spin system. The resulting x,y-magnetization rotating around the magnetic field axis z is detected as a function of time, the acquisition time t_2, and stored in the computer memory. By a Fourier transform with respect to t_2 the intensities and frequencies of the normal 1D spectrum are calculated by the computer within a few seconds. The greater the number M of data points used in the experiment, the better is the digital resolution of the spectrum measured in Hz per data point.
In a 2D experiment two or more pulses are applied for the preparation of the spin system during a first time domain, called evolution time t_1, before the free induction decay FID is acquired during t_2. In addition, the timing of the pulses and hence the evolution period t_1 is systematically incremented, thus N subsequent FID's are now acquired instead of only one. In practice N is chosen mostly between ca. 50 and 1000 depending on the type of experiment and the desired resolution. It is clearly evident that if the number of experiments and the digital resolution is not kept reasonably small the storage requirement M * N of the data matrix as well as the acquisition and processing times may be excessive. The processing consists of two consecutive steps. First, N subsequent Fourier transforms of all the rows of the data matrix are performed with respect to t_2 yielding a set of N spectra. Since t_1 was systematically incremented the amplitudes and phases of a specific signal in subsequent rows can also vary as a function of t_1, i.e. the signal along a specific column may be modulated e.g. by spin couplings, either directly (J-resolved 2D) or indirectly due to transfer of polarization between coupled spins (correlated 2D spectroscopy, COSY). The frequencies f_1 involved in the amplitude variation of the different columns are calculated by subsequent Fourier transforms with respect to t_1. In general, a magnitude calculation of the data is performed to obtain only positive intensities. The result, namely the intensities as a function of the two frequencies f_1 and f_2, is called a 2D spectrum. It can be presented as an impressive stacked plot as shown in Fig. 4. Here, a section of a proton-proton chemical shift correlated 2D spectrum is shown. The two axes cover the range between δ = 6.1 and 6.8 ppm and thus contain the chemical shift range of all olefinic protons except one (H(10')). The normal spectrum is concentrated along the diagonal running from top-right to bottom-left. In this homonuclear COSY spectrum, which is symmetrical with respect to the diagonal, cross-peaks at coordinates δ_A in f_1 and δ_B in f_2 (as well as δ_B in f_1 and δ_A in f_2)
reflect the fact that the two protons at chemical shifts δ_A and δ_B are spin-coupled to each other. Stronger couplings generally give more intense cross-peaks. This spectrum will be discussed later in more detail.
A stacked plot is not normally suited for extracting the information contained in a 2D spectrum, but it gives a good picture of the different intensities and the achieved signal-to-noise ratio. The information is much better revealed by so-called contour plots where the intensities are shown as closed contour levels of equal intensity, starting from a suitably chosen minimum level above the noise and incrementing normally by a factor of 2 from level to level.

J-resolved 2D - In this relatively simple 2D technique only the chemical shift information is retained in the horizontal f_2-axis, the coupling information solely along the perpendicular f_1-axis. It appears as if the spin multiplets were simply rotated by 90° into a second frequency axis. The technique can be applied to homonuclear (mostly proton-proton) and heteronuclear (mostly carbon-proton) systems. Two examples of the former were already discussed previously (Ref. 1). It is felt that the homonuclear variant will not find many useful applications in the field of carotenoids, because severe difficulties are encountered in strongly coupled spin systems.
More useful in specific cases is the heteronuclear J-resolved 2D experiment, an example of which is shown in Fig. 5. Here, the contour plot of the ^{13}C-^{1}H J-resolved 2D of ethyl 8'-apo-ß-caroten-8'-oate is presented on bottom. Since the width of the horizontal f_2-axis is more than 18 kHz according to the wide range of ^{13}C chemical shifts, the single contour lines representing the different intensities levels are, unfortunately, not resolved in this picture. The perpendicular f_1-axis containing the coupling information covers a range of 290 Hz. Although 128 experiments from 128 different t_1 increments were performed the digital resolution in f_1 (after zero-filling to 256 points) was only 1.1 Hz per data point. This is more than sufficient clearly to distinguish the different singlets, doublets, triplets and quartets in the contour plot but is insufficient for the detection of very small long-range couplings.

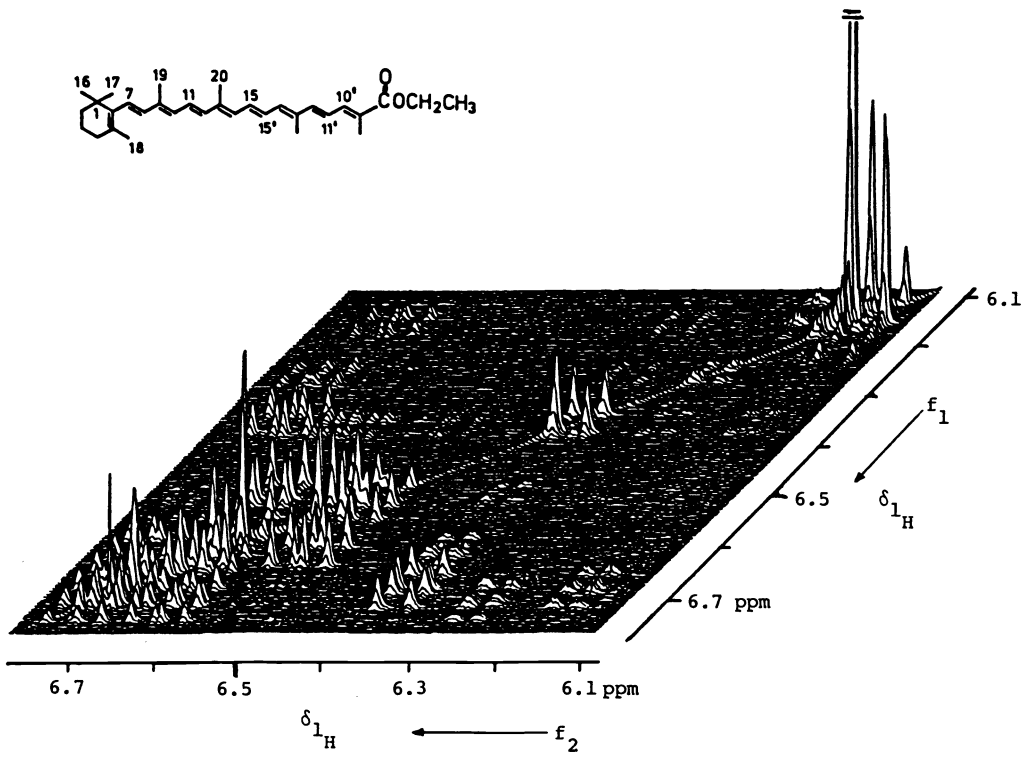

Fig. 4. Stacked plot (section between 6.1 and 6.8 ppm) of the symmetrized proton-proton chemical shift correlated 2D (400 MHz, COSY-90, N-type) of ethyl 8'-apo-ß-caroten-8'-oate (22 mg in 0.4 ml $CDCl_3$). Experimental data: Spectral width W 601.7 x 601.7 Hz, 2K x 470, zero-filled to 1K, 470 t_1 increments, 0.6 and 0.6 Hz per data point, polarization transfer delay 0.1 sec, relaxation delay 2.3 sec, 16 scans and 1 dummy scan per increment, sine-bell windows, magnitude spectrum, 9.5 h acquisition time, 1024 K file size. A corresponding contour plot is shown in Fig. 7.

The actual measurement of the resolved couplings and the visual presentation of the different multiplets can be achieved in the following way. First, a horizontal projection of the 2D spectrum is calculated (see top of Fig. 5). It looks very similar to the usual broad-band decoupled ^{13}C spectrum but its digital resolution is, in general, necessarily smaller (here 9 instead of ca. 1 Hz per point). Since the maxima of the horizontal projection represent the chemical shift of the different carbons, the corresponding multiplets can be plotted as so-called J-cross-sections as normal intensity plots along the f_1-axis. All J-cross-sections (except COO) which were resolved are shown in Fig. 6 together with the assignments, the intensity scaling factor, and the chemical shifts. In carotenoids the $^1J_{CH}$-values of olefinic carbons are in a rather narrow range between ca. 149 and 155 Hz and, therefore, they are not very useful for the purpose of assignment. However, the number of long-range couplings or the width of the unresolved components of a multiplet can be rather characteristic. Thus C(7), C(11) and the corresponding C(11') usually appear as sharp doublets with high intensities. They can already be distinguished from other carbons by inspection of the horizontal projection as seen in Fig. 5.

A further point should be noted here. If a singlet and a doublet appear at (almost) the same chemical shift they can be completely separated in a J-resolved spectrum as is seen from two examples in Fig. 6. The intensities and the magnitude of the measured J_{CH}-coupling allows a safe differentiation from a single triplet signal.

It is evident from this example that any meaningful application of this special 2D method will be essentially limited to those cases where the number and magnitude of the carbon-proton couplings are of importance for the solution of a structural problem and the normal ^1H-coupled ^{13}C-spectrum is too crowded for a clear-cut differentiation.

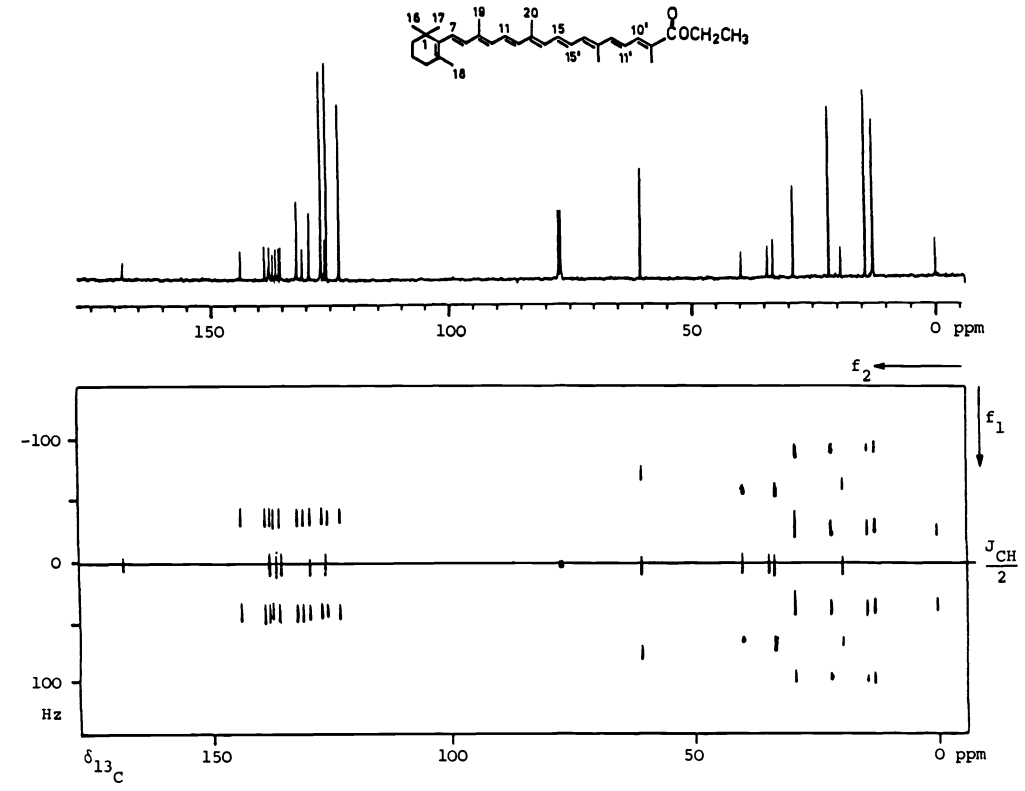

Fig. 5. Ethyl 8'-apo-ß-caroten-8'-oate (100 mg in 0.5 ml $CDCl_3$): Contour plot and horizontal projection of the ^{13}C-^{1}H J-resolved 2D spectrum. Experimental conditions: W 18518 x 290 Hz, 4K x 128 data points, zero-filled to 256 points, 128 t_1-increments, digital resolution 9 and 1.1 Hz, 3.5 sec. relaxation delay, sine-bell windows, magnitude spectrum, file size 512 K, ca. 14 h acquisition time.

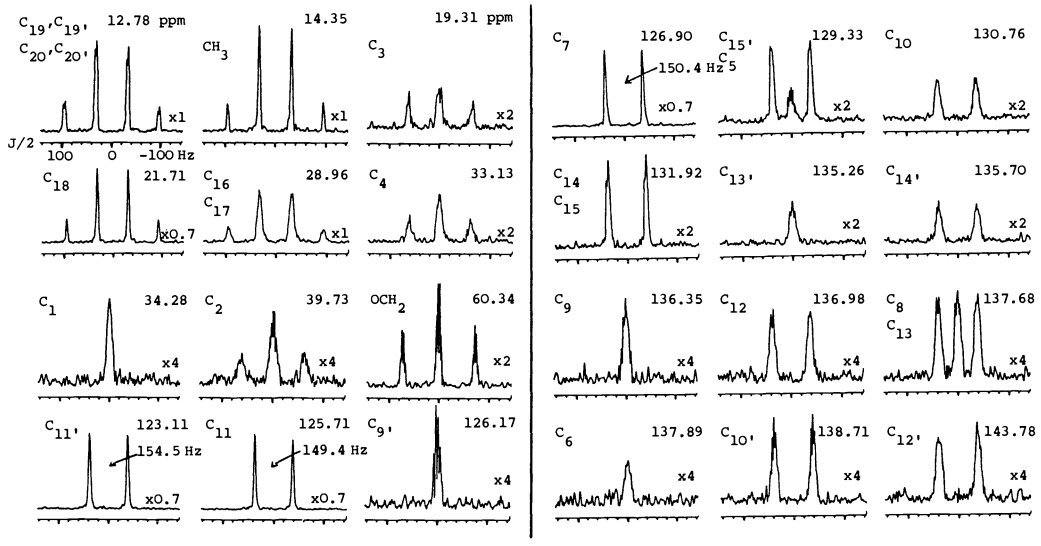

Fig. 6. J-cross-sections of the J-resolved 2D spectrum of Fig. 5. The assignments are given together with the chemical shifts and the intensity scaling factors. The COO-signal is not shown.

Homonuclear chemical shift correlated 2D spectroscopy (COSY) - In this experiment a spin coupling between two protons is revealed by the existence of cross-peaks in the 2D plot (Ref. 14). Since it is actually the homonuclear spin coupling which causes the cross-peaks the method is also called homoscalar correlated 2D. It is often possible to derive the full sequence of coupled protons even in a complicated compound, thus providing important information on its molecular structure. As will be shown the coupling pathway or connectivity of protons can even in such cases be detected where the couplings are very small. The previous 400 MHz COSY spectrum of Fig. 4 from ethyl 8'-apo-ß-caroten-8'-oate is now presented in Fig. 7 as a contour plot which is much more appropriate for the deduction of the connectivities. Since the olefinic part is highly crowded a very good digital resolution of only 0.6 Hz per point was used. The normal 1D spectrum and the assignments are given in the upper 1D spectrum. The 2D contour plot is symmetrical with respect to the diagonal on which the normal spectrum is seen. Those peaks which are very close to the diagonal are caused by transfer of magnetization between the transitions of the same proton. Thus, the doublets appear as 2x2, all doublets of doublets as 4x4 signals. More distant from the diagonal are found the cross-peaks indicating that the two corresponding protons are coupled to each other. Thus, the two off-diagonal peaks at coordinates (δ_A,δ_B) and (δ_B,δ_A) prove the presence of a J-coupling between proton A at (δ_A,δ_A) and B at (δ_B,δ_B). One of the advantages of a COSY in the case of highly crowded signals near the diagonal is the fact that the multiplet structures can be derived by inspection of the cross-peaks which are often sufficiently separated.
If a good signal-to-noise ratio has been achieved in a COSY spectrum by application of a longer accumulation time it is often possible to detect very weak cross-peaks due to long-range couplings. As will be seen later in this COSY spectrum a long-range coupling of the order of 0.1 Hz or less extending over 7 intervening bonds can be detected although such small couplings can not normally be seen or resolved in the 1D spectrum. In Fig. 7 all long-range connectivities were designated in the upper-left triangle, the 3-bond connectivities in the lower-right triangle of the symmetrical 2D spectrum.
The procedure for revealing the sequences of coupled protons can start e.g. from the isolated signal of H(10') at lowest field. Horizontal and vertical lines lead to the strong cross-peaks with H(11'), the diagonal signal of which is now found at the intersections of the horizontal and vertical lines with the diagonal. A further much weaker cross-peak due to $^4J_{10',12'}$ identifies the signal of H(12'). It can also be located from the much stronger, direct cross-peaks between H(11') and H(12') via $^3J_{11'12'}$. Further connectivities are visible between H(15), H(15') and H(14), between H(11), H(12) and H(10), between H(15') and H(14') etc. Some further long-range connectivities are marked in the upper-left triangle of Fig. 7. Interestingly, a cross-peak H(15)/H(11') is clearly visible, corresponding to a 7-bond coupling between these two protons (see also Fig. 8). From the 2D spectrum of Fig. 7 the whole sequence of protons between H(10) and H(10') is deduced. The connectivity between H(7) and H(8) can also be found in an expanded plot of the right upper corner (not shown) although their chemical shifts are very close to each other.
A very convenient way of visualizing the different connectivities is to plot selected rows (or columns) of the 2D data. Three selected rows chosen at 6.59 ppm through H(12'), at 6.74 ppm through H(15') and 7.30 ppm through H(10') (see arrows in Fig. 7) are presented as examples in Fig. 8. The form and intensities of the diagonal peak and its cross-peaks are clearly seen as well as the above-mentioned long-range connectivity.
In a completely analogous way the connectivities between the protons of in-chain methyl groups and olefinic protons are detectable if the experiment is run with a spectral width covering the whole spectrum. However, in this case the digital resolution has to be reduced in order to avoid an excessive size of the data matrix. Despite several drawbacks of this technique, namely long accumulation and processing times and large data storage requirements, it is strongly recommended for the solution of complex structural problems if simpler methods such as DID cannot provide all necessary information.

Heteronuclear chemical shift correlated 2D - This technique (Ref. 15) which is mostly applied to carbon-13 and protons is even more useful in practice since it provides connectivities between ^{13}C and ^1H chemical shifts. The two portions of a heteronuclear 2D from (5'R)-cryptocapsone are presented in Fig. 9 and 10, showing separately the olefinic-olefinic and the aliphatic-aliphatic sections of the same experiment. The proton spectrum runs along the vertical f_1-axis, the carbon spectrum along the horizontal f_2-axis. For convenience, both 1D spectra of the two nuclei and the horizontal projection of the 2D spectrum are also presented. Since the delay for polarization transfer between the two nuclei was chosen to enhance connectivities by one-bond couplings of 140 Hz, cross-peaks are seen only between carbons and their directly attached protons. Correspondingly, in the horizontal projections only signals of protonated carbons are detectable. Thus, starting from a known proton signal in f_1 one obtains in a simple and mostly unambiguous way the assignment of the corresponding carbon in f_2. In a strongly crowded proton spectrum it frequently suffices to know the relative order of the chemical shifts to assign the carbon signals. Conversely, if the carbon assignment is known the chemical shift of the coupled proton is deduced.

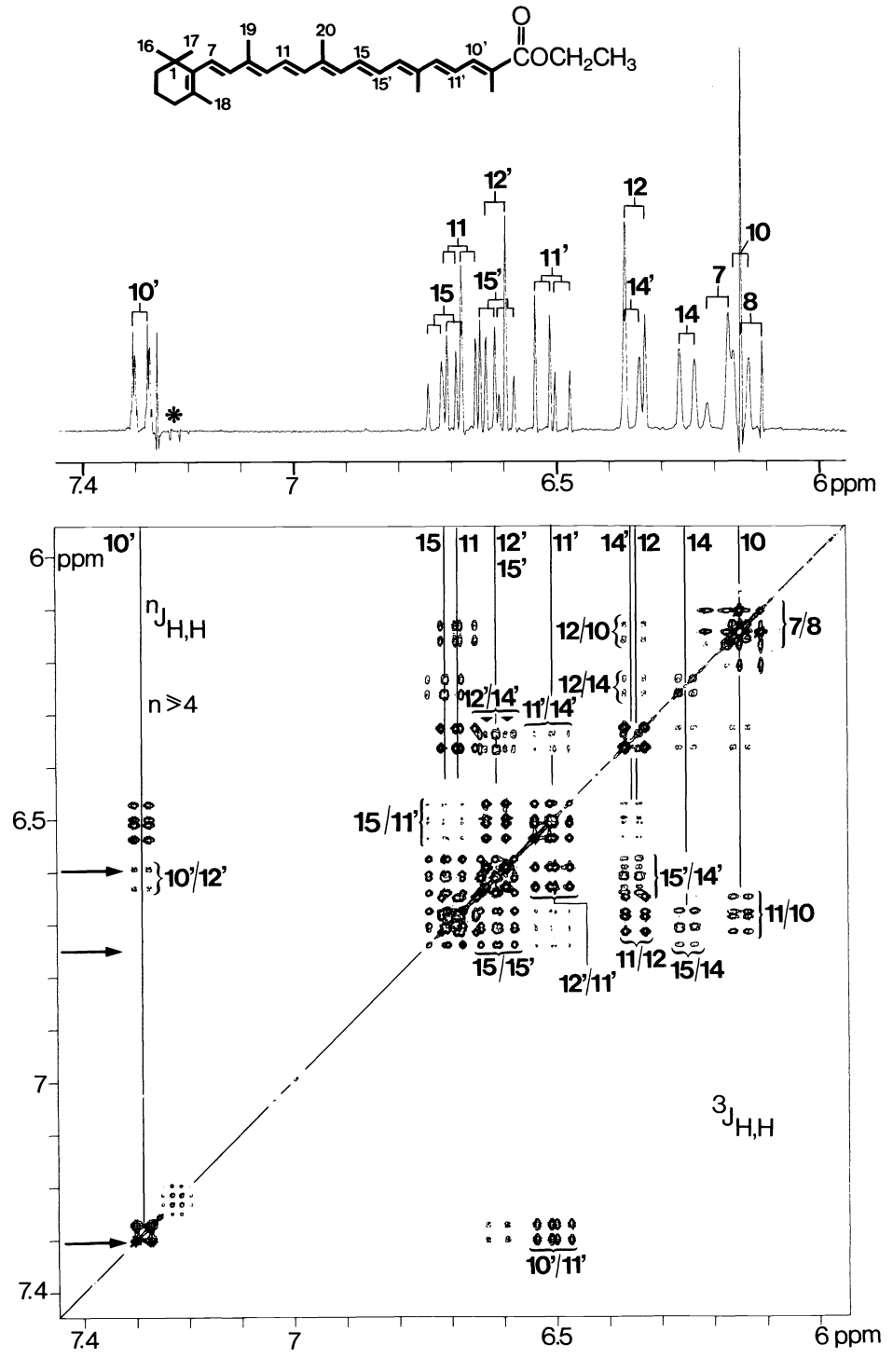

Fig. 7. Top: Olefinic range of the resolution enhanced 400 MHz ^{1}H-NMR spectrum of ethyl 8'-apo-ß-caroten-8'-oate. Bottom: Contour plot of the symmetrized COSY-90 spectrum. Experimental conditions see Fig. 4; * folded signal. Arrows indicate selected rows shown in Fig. 8.

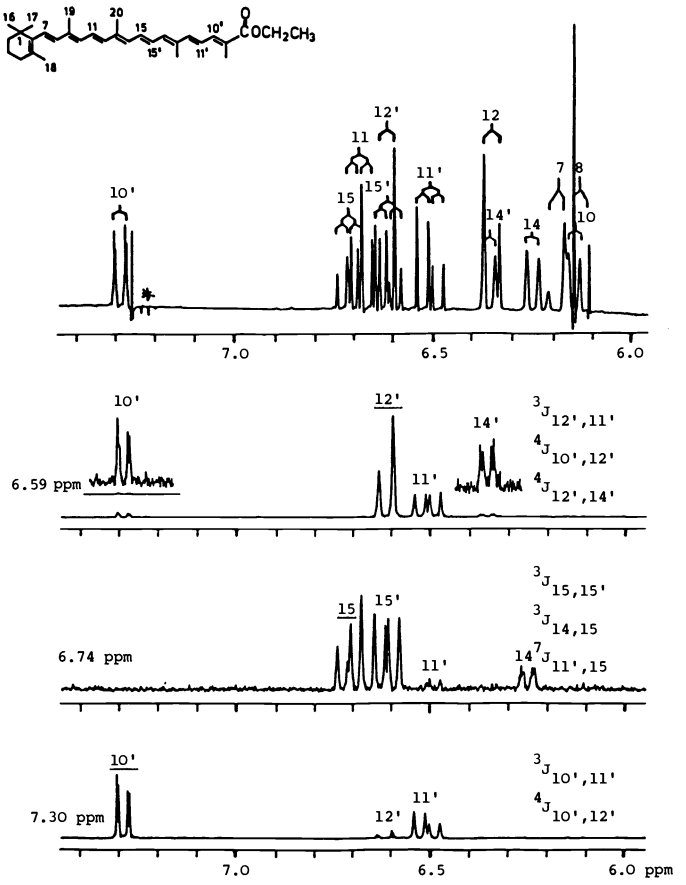

Fig. 8. Top: Olefinic section of the 400 MHz ^{1}H-NMR spectrum of ethyl 8'-apo-ß-caroten-8'-oate. Bottom: Selective horizontal rows of the COSY spectrum of Fig. 7 plotted at 6.59, 6.74 and 7.30 ppm (see arrows in Fig. 7) indicating all cross-peaks of $H_{12'}$, H_{15} and $H_{10'}$, respectively.

In the case of ambiguities important aid is given by additional plots of horizontal rows at selected proton chemical shifts, revealing the position of the connected carbon signal, or conversely, the plot of selected columns yielding the multiplet structure of the signal of the proton coupled to a specific carbon.

A very useful supplement to the one-bond coupling experiment is obtained by a subsequent experiment tuned to connectivities mediated by two- and three-bond couplings which are frequently between 5 and 10 Hz. This gives further relevant information since connectivities between more distant nuclei, including the quaternary carbons, are involved. As an example, the aliphatic-aliphatic portion of the ^{13}C-^{1}H correlated 2D of the same compound is shown in Fig. 11. The delay for polarization transfer was chosen to enhance cross-peaks caused by long-range couplings of ca. 8 Hz. However, some of the cross-peaks caused by the much larger one-bond couplings can be still detectable.

For purposes of interpretation it is important to note that only two- or three-bond carbon-proton couplings are sufficiently large to cause long-range cross-peaks. Applying this rule and the results from Fig. 10, all the cross-peaks of Fig. 11 can be readily assigned. It is evident that not only the assignments of proton and carbon signals can be deduced or confirmed, but also important information on the molecular structure is revealed by the connectivities caused by the two- and three-bond couplings. Thus, as an example, in this section of the 2D plot, protons H(16) and H(17) of the ß-ring have cross-peaks with C(2), C(1) and C(17), C(16); protons H(18) only with C(4) and C(18). In the 5-membered ring, on the other hand, protons H(16') and H(17') have cross-peaks with C(5'), C(2') and C(1'), protons H(18') with C(5'), C(4') and C(1').

Further relevant information of this type can be deduced from the other sections of the heterocorrelated 2D, namely the aliphatic-olefinic and olefinic-olefinic sections which are not shown here. This includes e.g. cross-peaks between H(19) and C(8), C(9) and C(10) as well as between H(20) and C(12), C(13) and C(14).

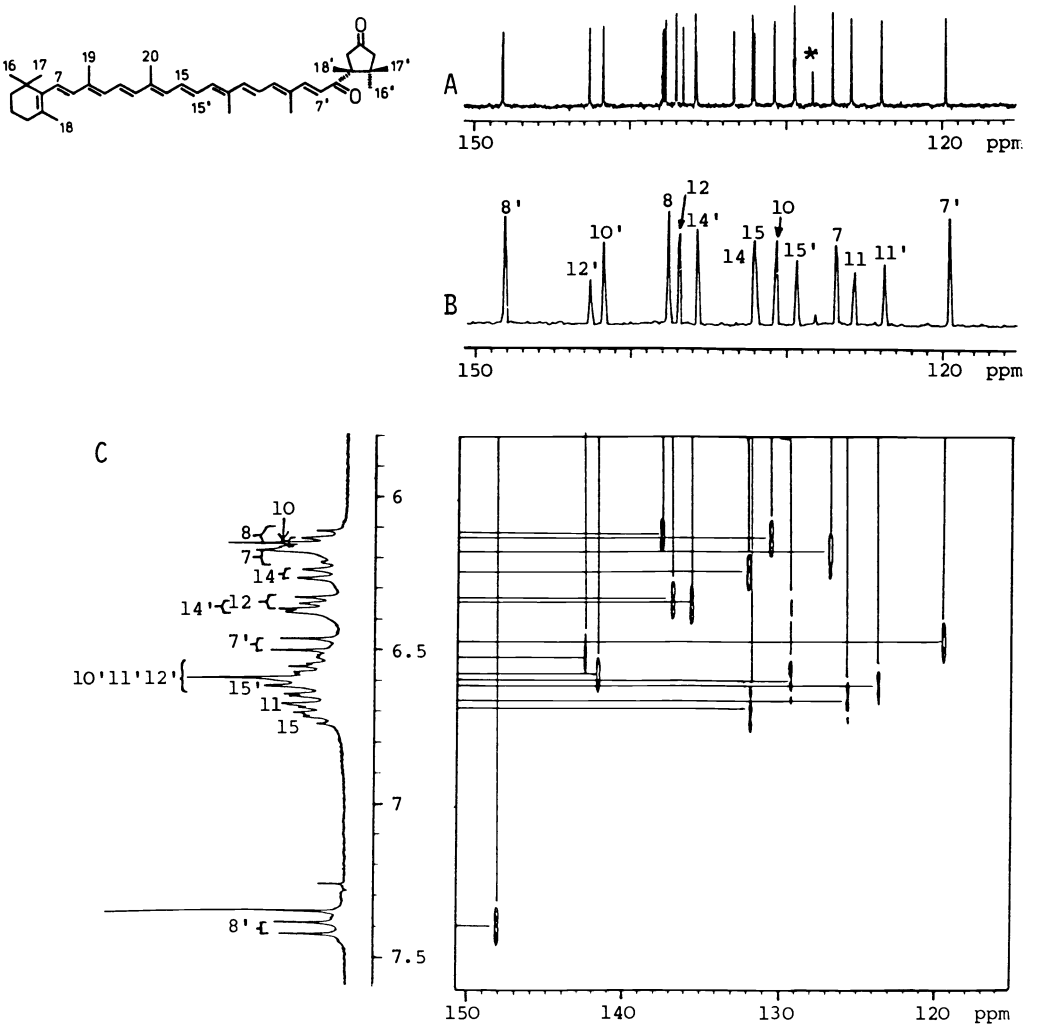

Fig. 9. A: 100 MHz ^{13}C-NMR spectrum (olefinic section) of (5'R)-cryptocapsone (45 mg in 0.5 ml $CDCl_3$); *impurity. B: Horizontal projection of the ^{13}C-^{1}H correlated 2D spectrum. C: 400 MHz ^{1}H-NMR spectrum measured with the decoupler coil. Bottom: ^{13}C-^{1}H correlated 2D spectrum (olefinic-olefinic section); Experimental conditions: W 21740 x 3334 Hz, 4K x 256, zero-filling to 512, 10.6 and 6.5 Hz per data point, 2.5 sec relaxation delay, polarization transfer delay 3.6 msec (J_{CH} ~ 140 Hz), 48 scans, 1 dummy scan, sine-bell windows, magnitude spectrum, 1024 K file size, 9 h acquisition.

In conclusion it is found that the heteronuclear chemical shift correlated 2D is extremely useful for the assignment of signals and the deduction of structural information on the nuclear framework and hence for the elucidation of molecular structures. In practice, we normally acquire both the one-bond and the long-range type of spectra in two subsequent experiments normally during an overnight run from about 20 to 50 mg of sample.

INADEQUATE-2D - This technique, also called Carbon-Carbon Connectivity (CCC), is a 2D variant of the former 1D-INADEQUATE experiment which was used to measure ^{13}C-^{13}C couplings constants in natural abundance (Ref. 16).
In normal ^{13}C-NMR the spectrum from molecules containing ^{13}C at ca. 1 % natural abundance is acquired. The probability of having two adjacent ^{13}C nuclei in a molecule is about 100 times less. Since two neighbouring carbons are spin-coupled the resulting two doublets have roughly 200 times smaller intensities. Despite this extreme loss of intensity

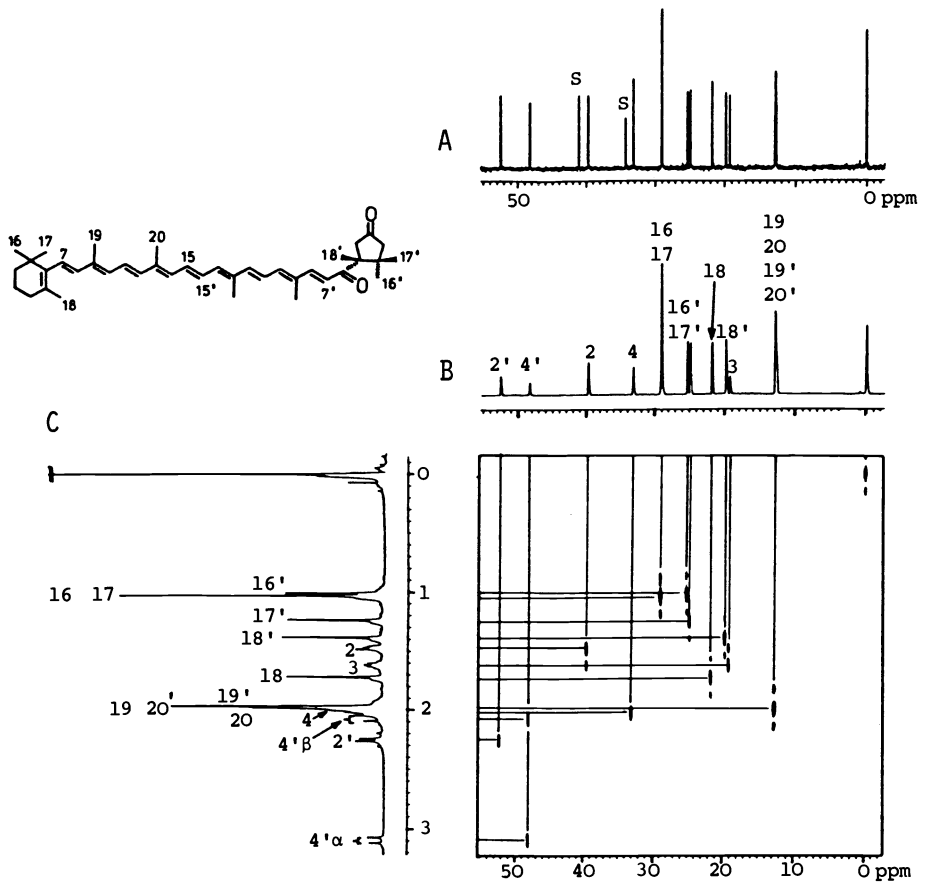

Fig. 10. Aliphatic-aliphatic section, continued from Fig. 9.

it is possible in favourable cases to acquire an INADEQUATE spectrum with a reasonable signal-to-noise if very long acquisition times can be accepted and sufficiently large sample quantities of several 100 mg are available and soluble in ca. 2 ml of solvent. In the 1D version, all the pairs of doublets are superimposed along the only frequency axis f_2. Furthermore, the much more intense singlet signals of molecules with only one carbon-13 are partly superimposed because they are mostly incompletely suppressed by application of complicated phase cycles.

In the 2D-INADEQUATE the different AB or AX spectra are separated along the second frequency axis f_1 according to their so-called double quantum frequency. This is the sum of their frequency distances from the transmitter frequency which is normally placed in the middle of the f_2-axis.

An example, using a quite useful experimental variant called refocused 2D-INADEQUATE (Ref. 17), is shown in Fig. 12. It was obtained from 640 mg of astaxanthin diacetate with an acquisition time of 64 hours. This long acquisition time is mainly caused by the fact that a relaxation delay of (at least) 2.5 sec had to be interleaved after each scan because the ^{13}C spin lattice relaxation time T_1 of the unprotonated carbons of this compound can exceed 3 sec (Ref. 1). An average value for J_{CC} of 55 Hz was adopted for this measurement although the actual coupling constants vary between roughly 35 and 65 Hz. The pairs of doublets are symmetrically displaced with respect to the diagonal. This simplifies the identification of the different connectivities and, in addition, artifacts having no symmetrical counter-parts can be removed by symmetrization. Unfortunately, the doublets are very poorly resolved in this picture since the total range of f_2 covers 20.8 kHz. On the diagonal some stronger residual artifacts are seen which are caused by imperfectly suppressed singlets of slowly relaxing carbon-13 nuclei.

The connectivities of the carbon-carbon skeleton are revealed by the procedure shown in Fig. 12. Thus, starting e.g. from the quaternary carbon C(1), its neighbours C(17), C(16), C(2) and C(6) are clearly revealed by the existence of the corresponding pairs of doublets. Similarly, C(2) is connected to C(3), C(3) to C(4), C(4) to C(5), C(5) to C(6), and so forth. The CCC is interrupted at C(9)/C(10), which have almost identical chemical shifts,

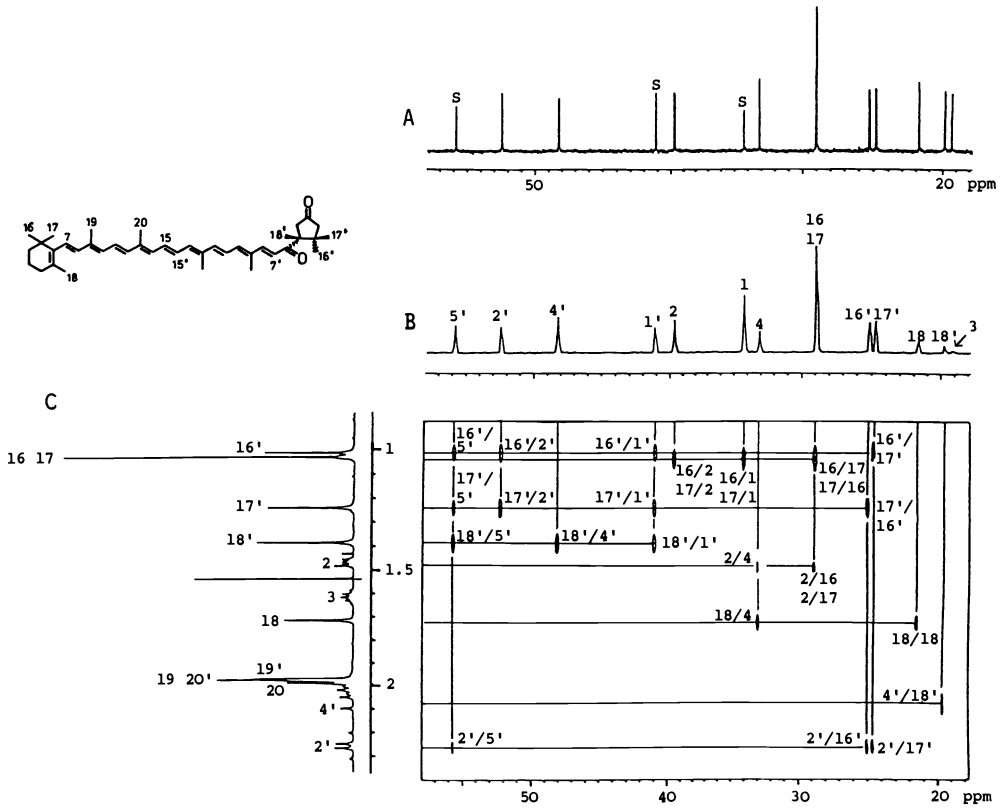

Fig. 11. (5'R)-cryptocapsone, aliphatic sections of the 100 MHz ^{13}C-NMR (A), the horizontal projection (B) of the ^{13}C-^{1}H correlated 2D (bottom-right). C: aliphatic section of the 400 MHz ^{1}H-NMR. Polarization transfer delay chosen to enhance long-range couplings $^{1}J_{CH} \sim {}^{3}J_{CH} \sim 8$ Hz. Other experimental conditions as in Figs. 9 and 10.

and at the intervening oxygen to the substituent at C(3). The position of the acetyl group is, however, evidenced by consideration of the chemical shift. This example clearly demonstrates the great power of this 2D method to reveal in a fully unambiguous way not only all the assignments but also the full sequence of carbons in the molecular structure including ring size, position of double bonds and of methyl groups. It should be mentioned that experiments with reduced sample quantities or reduced accumulation time of the order of 24 h can also be quite useful. However, in this case only connectivities between protonated carbons with short relaxation times are likely to be detected as e.g. the olefinic carbons with T_1's of 0.3 sec or less.

CONCLUSION

From these selected examples it is clearly evident that NMR spectroscopy has again made some steps forward increasing its power and utility for the solution of structural problems in the field of carotenoids. Although some of the recent 2D techniques have become increasingly complex and sophisticated, there is no doubt that they will be more and more applied even on a routine basis. All the experiments described here were performed in a fully automated manner under computer control on a Bruker WM 400 FT NMR spectrometer using standard software.

Acknowledgement -I am indebted to several colleagues who provided the compounds used in this study. I should like to specifically mention Drs. K. Bernhard, H. Mayer, A. Rüttimann, E. Widmer, R. Zell and Mrs. K. Schiedt. Thanks are also due to Mr. W. Grunauer for his skilful technical assistance.

REFERENCES

1. G. Englert, in Carotenoid Chemistry & Biochemistry, G. Britton and T.W. Goodwin, Editors, Pergamon Press, 107-134 (1982).
2. E. Märki-Fischer, P.-A. Bütikofer, R. Buchecker, and C.H. Eugster, Helv. Chim. Acta 66, 1175-1182 (1983).

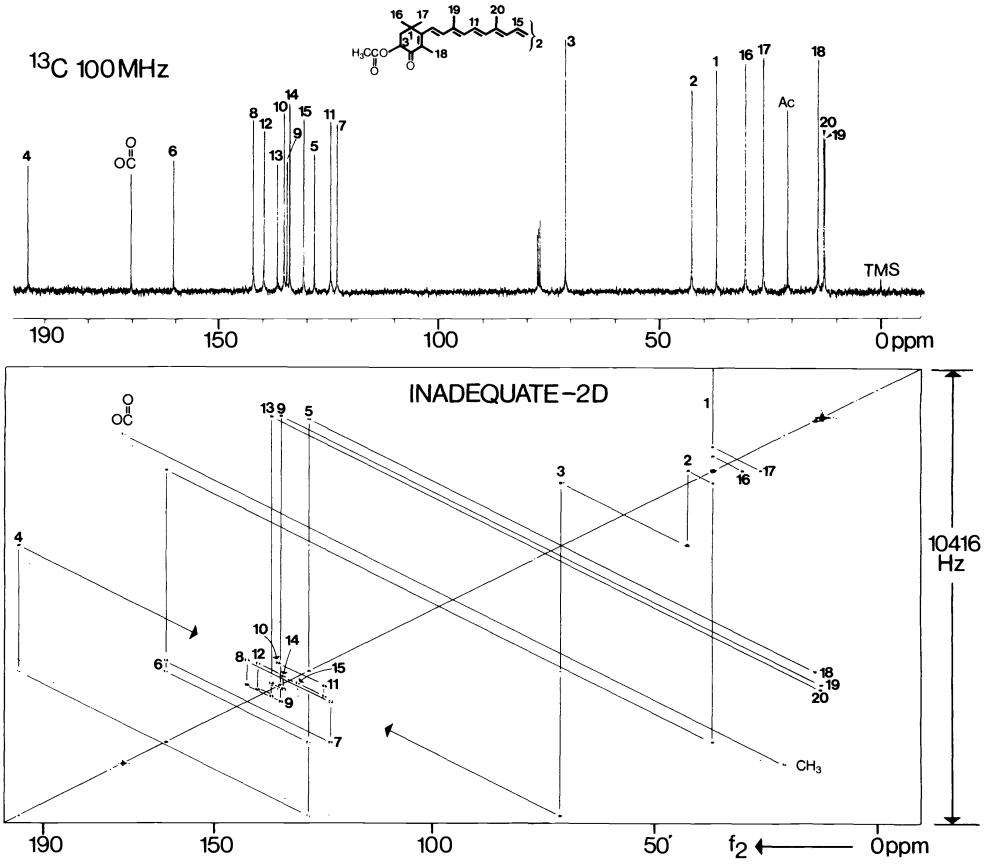

Fig. 12. Top: 100 MHz ^{13}C-NMR spectrum of astaxanthin diacetate. Bottom: Contour plot of the symmetrized, refocused 2D-INADEQUATE. The carbon connectivities are indicated starting from C(1). Experimental conditions: 640 mg in 1.8 ml $CDCl_3$, W 20.8 x 10.4 kHz, 4K x 256, zero-filling to 2K, 10.2 and 5.1 Hz digital resolution, relaxation delay 2.5 sec, echo-delay 4.5 msec (J_{CC} = 55 Hz), ^{13}C pulses 90° (14 μsec), 180° and 120°, Lorentz-to-Gauss filtering, LB = -4, GB = 0.1, LB1 = -4, GB1 = 0.1, 320 scans per t_1-increment, 4096 K data file, acquisition time 64 h.

References (contd.)

3. E. Märki-Fischer, R. Buchecker, C.H. Eugster, G. Englert, K. Noack, and M. Vecchi, Helv. Chim. Acta 65, 2198-2212 (1982).
4. W. Eschenmoser, P. Uebelhart, and C.H. Eugster, Helv. Chim. Acta 66, 82-91 (1983).
5. G. Englert, Helv. Chim. Acta 58, 2367-2390 (1975); K. Bernhard, G. Englert, H. Mayer, R.K. Müller, A. Rüttimann, M. Vecchi, E. Widmer, and R. Zell, Helv. Chim. Acta 64, 2469-2484 (1981).
6. A. Rüttimann, G. Englert, H. Mayer, G.P. Moss, and B.C.L. Weedon, Helv. Chim. Acta 66, 1939-1960 (1983).
7. K.G.R. Pachler and P.L. Wessels, J. Chem. Soc., Chem. Commun., 1038-1039 (1974).
8. H. Kessler, G. Krack, and G. Zimmermann, J. Magn. Res. 44, 208-211 (1981).
9. G.A. Morris and R. Freeman, J. Am. Chem. Soc. 101, 760-762 (1979).
10. D.M. Doddrell, D.T. Pegg, and M.R. Bendall, J. Magn. Res. 48, 323-327 (1982).
11. O.W. Sørensen and R.R. Ernst, J. Magn. Res. 51, 477-489 (1983).
12. M.R. Bendall, D.T. Pegg, D.M. Doddrell, S.R. Johns, and R.I. Willing, J. Chem. Soc., Chem. Commun., 1138-1140 (1982).
13. J. Jeener, Ampere International Summer School, Basko Polje, Yugoslavia (1971).
14. A. Bax, Two-Dimensional Nuclear Magnetic Resonance in Liquids, Delft University Press, D. Reidel Publishing Company, Boston, London (1982); R. Benn and H. Günther, Angew. Chem. 95, 381-411 (1983).
15. A.A. Maudsley and R.R. Ernst, Chem. Phys. Lett. 50, 368-372 (1977).
16. A. Bax, R. Freeman, and S.P. Kempsell, J. Am. Chem. Soc. 102, 4849-4851 (1980).
17. D.L. Turner, J. Magn. Res. 49, 175-178 (1982).